Schachman, H. K., Adler, J., Radding, C. M., Lehman, I. R., and Kornberg, A. (1960), *J. Biol. Mol. 235,* 3242.
Simon, M., Ohki, I., Chang, H. C., Lohr, K., and Laskowski, M., Sr. (1970), *Biochim. Biophys. Acta 224,* 253.
Skinner, D. (1967), *Proc. Natl. Acad. Sci. U.S.A. 58,* 103.
Szybalski, W., Kubinski, H., and Sheldrick, P. (1966), *Cold Spring Harbor Symp. Quant. Biol. 31,* 129.
Tsuboi, M. (1964a), *Biopolym. Symp. 1,* 527.
Tsuboi, M. (1964b), *J. Polymer. Sci. 7,* 125.
Tsuboi, M. (1970), *Appl. Spectrosc. Rev. 1,* 45.
Tsuboi, M., Matsuo, K., and Nakanishi, M. (1968), *Biopolymers 6,* 123.
Wells, R. D., Larson, J. E., Grant, R. C., Shortle, B. E., and Cantor, C. R. (1970), *J. Mol. Biol. 54,* 465.
Yamagashi, H., and Takahashi, I. (1971), *J. Mol. Biol. 57,* 369.

Conformations and Interactions of Histone H2A (F2A2, ALK)†

E. M. Bradbury, P. D. Cary, C. Crane-Robinson,* H. W. E. Rattle, M. Boublik,‡ and P. Sautière§

ABSTRACT: Conformational changes in histone H2A (ALK, F2A2, IIb1) as a function of ionic strength and pH have been followed using high resolution nuclear magnetic resonance (NMR), circular dichroism (CD), and infrared (ir). While change in pH from 3 to 7 (no added salt) causes little structural change, added salt induces the formation of both α helix (28% maximum) and intermolecular associates in the region of the molecule between 25 and 113. No β structure was observed at high salt. By the use of different salts it was shown that the structural changes were due largely to nonspecific counterion screening by the added anion. Comparison of observed with simulated NMR spectra has led to the proposal that an ionic strength dependent equilibrium exists between largely unstructured coil molecules and fully structured and aggregated molecules. NMR spectra of H2A obtained in the presence of DNA showed that both the N- and C-terminal regions bind to DNA, i.e., not the portion of the chain that is involved in interhistone interactions.

The sequence determinations of histones[1] H4 (F2A1), H2A (F2A2), H2B (F2B), and H3 (F3) and the partial sequence and compositions of peptides of H1 (F1) listed in Croft (1973) have all shown that histones have a marked asymmetry in the distribution of amino acids along the polypeptide chains. All histone sequences contain well-defined regions which are rich in basic residues and the helix destabilizing residues proline, serine, and glycine. The regions complementary to these basic segments contain a high proportion of the helix favoring apolar residues, aromatic, acidic residues, and relatively few basic residues. These factors have led to the suggestion that the basic segments are the primary sites for interactions with DNA while the apolar segments contain the potential for secondary conformations and act as sites for histone–histone or for other chromosomal–protein interactions. Evidence for these interactions has been obtained from high-resolution nuclear magnetic resonance (NMR) studies of histones H1, H4, and H2B (Boublik et al., 1970a,b; Bradbury and Rattle, 1972).

The nonuniformity in the distribution of residues in the calf thymus H2A sequence (Yeoman et al., 1972; Sautière et al., 1974) is shown in Table I which gives the composition of each quarter of the molecule. The amino quarter 1–32 is very basic with a net positive charge of +10, contains 10 helix-destabilizing residues (glycine + serine + proline), and only three of the apolar residues, leucine, valine, and isoleucine. (The division of residues into the three categories helix breaker, indifferent, and helix forming is given, for example, in Lewis and Scheraga, 1971.) In contrast the second quarter 33–65 contains only three basic residues which together with four glutamic acid residues gives a net negative charge of −1; it contains four helix destabilizing residues and 11 apolar residues. The third quarter has a similar character to the second though the net charge is +3. The final quarter is mixed, having an apolar nature from 98 to 116 (eight apolar and no basic residues), while from 117 to 129 it is very basic with six lysines and three helix destabilizing residues. A more detailed analysis of sequence-conformation relations is to use the predictive methods developed by Scheraga and his coworkers. These have been applied to histones (Lewis and Bradbury, 1974) and in the case of calf H2A (Figure 1) at neutral pH the plot of the probability that residue i is helical against the residue number i contains a strong maximum between residues 47 and 67 with a weaker maximum in the region of residue 84. The

† From the Biophysics Laboratories, Department of Physics, Portsmouth Polytechnic, Gun House, Hampshire Terrace, Portsmouth P01 2QG, United Kingdom. *Received July 29, 1974.* This research is supported by the Science Research Council of Great Britain.

‡ Present address: The Roche Institute of Molecular Biology, Nutley, New Jersey.
§ Present address: Institut de Recherches sur le Cancer, Lille, France.

[1] The new histone nomenclature used here was accepted by the participants at the CIBA Foundation Symposium on the Structure and Function of Chromatin, April 3–5, 1974. This new nomenclature which has been proposed to the appropriate international nomenclature committee is as follows for each histone, where the previous names are given in parentheses: H1 (F1, I, KAP); H2A (F2A2, IIb1, ALK); H2B (F2B, IIb2, KSA); H3 (F3, III, ARK), H4 (F2A1, IV, GRK), and H5 (F2C, V, KAS).

predicted helical region lies in the center of the molecule from 47 to 93, i.e., 47 residues. Other predictive schemes for secondary structure can also be used for this molecule. That of Chou and Fasman (1974) is readily applied and leads to the following predicted helical regions: 9–17, 29–36, 40–45, 51–67, 81–88, 90–98, and 121–127. However, both 9–17 and 121–127 are highly charged regions containing many lysine and arginine residues and on this account are not expected to be helical. The remaining regions sum to 48 residues. The latest methods of Ptitsyn, Finkelstein, and Lim (see, for example, Ptitsyn et al., 1973) have also been applied for us by those authors to the H2A molecule and they predicted 3 helical segments, 26–36, 48–66, and 91–101: a total of 41 residues. These two predictions are displayed in Figure 1 along with that of Lewis and Bradbury. It can be seen that there is a fair measure of agreement between the three methods particularly as regards the central region 48–67. On the basis of the circular dichroism (CD) data, however (see below), one can conclude that there is a degree of overprediction in all of them. Predictions of β structure have not been carried out since this conformation is demonstrated by ir spectroscopy (see below) to be absent.

High-resolution NMR has proved a very powerful technique for studying the interactions of histones. The main reason for this is to be found in the asymmetric distributions of residues in histones, described above. Thus when conformational changes and interchain interactions are induced in histones by increasing the ionic strength of aqueous solutions the segments involved can be unambiguously identified from changes in the NMR spectra. There are two basic assumptions involved in these studies. The first is that increasing the ionic strength of aqueous solutions induces conformational changes and interhistone interactions similar to those found in the ionic environment of DNA. This assumption can be verified only when interactions of histones in chromatin can be studied. The second assumption is that marked apparent loss in area of only certain resonance peaks (when compared to other peaks in the same spectrum) is due to dipolar broadening, i.e., faster relaxation and shorter T_2 values, as a result of restricted motions of specific regions of the polypeptide chain consequent upon interchain interactions. Since histone molecules consist of single polypeptide chains and paramagnetic ions are excluded from the system, the second assumption is most probably valid. Thus while the CD spectrum reflects changes in the intramolecular secondary structure of individual molecules, the broadening of NMR resonances is a consequence of intermolecular interactions that lead to increased molecular weights and longer tumbling times in solution.

Materials and Methods

(*i*) *Histone H2A.* Histones were extracted from calf thymus using Johns method II (1964). Ethanol-HCl was used to extract histone H3 and then F2A (an H2A/H4 mixture) was precipitated with acetone-HCl. The F2A mixture was separated into histone H4 and histone H2A using Johns' method (1967). Good purification was achieved by working at one-half the recommended histone concentration. This left histone H4 in a pure state and histone H2A slightly contaminated by histone H2B and histone H3. The impurities were avoided by taking only the first parts of the H2A precipitating from the solution and recycling the precipitate until the acrylamide gel showed only a single sharp band. The H2A as hydrochloride was washed several times with acetone and dried under vacuum at room temperature. The sea urchin histone H2A (ALG) was extracted by one of us (P.S.) from the gonads of *Psammechinus miliaris* and purified initially using ion-exchange chromatography on Biorex 70 and finally by gel filtration on Sephadex G-100 (Wôuters-Tyrou et al., 1974).

Table I: Histone H2A Composition.

	Residue No.			
	1–32	33–65	66–97	98–129
Leucine	1	7	5	3
Isoleucine	0	1	3	2
Valine	2	3	0	3
Alanine	4	6	4	3
Lysine	4	1	3	6
Arginine	6	2	4	0
Glutamic acid	0	4	2	1
Aspartic acid	0	0	2	0
Glycine	6	3	1	4
Serine	3	0	0	1
Proline	1	1	1	2
Threonine	1	1	1	2
Glutamine	2	0	1	2
Asparagine	0	1	4	1
Phenylalanine	1	0	0	0
Tyrosine	0	3	0	0
Histidine	1	0	1	2
Net charge (pH 7)	+10	−1	+3	+5
Helix Destabilizers	10	4	2	7

Solutions of H2A for spectroscopy were made up by dissolving solid protein in water. The pH was adjusted with DCl or NaOD and microliter quantities of salt solutions were added in steps to change the ionic strength. In the case of spectra obtained in urea (Figure 6), a separate solution was used for each spectrum. The protein was dissolved initially in a urea solution of the correct strength and phosphate buffer was added to the appropriate concentration. In none of the protein solutions studied was any precipitation or cloudiness noted. In the studies of H2A/DNA interactions, the solutions at 0.8 *M* NaCl (Figure 12) were markedly turbid.

(*ii*) *Circular Dichroism.* CD spectra were obtained on a Cary 61 instrument using path lengths from 5 to 0.1 mm and protein concentrations from 0.05 to 5 mg/ml.

(*iii*) *High Resolution NMR.* Proton NMR spectra were obtained at 270 MHz using a superconducting Bruker WH 270 spectrometer operating in the Fourier transform mode. Typical conditions of observation were: an interval between pulses (60–70°) of 1 sec, data collection over 0.5 sec, and multiplication of the free induction decay by an exponential equivalent to line broadening to about 2 Hz.

(*iv*) *Infrared.* Ir spectra were obtained on a Grubb Parsons Spectromaster having an effective resolution of about 3 cm^{-1}. A 25-μ path-length barium fluoride cell was used.

Results

All the measurements described below have been performed on calf thymus H2A, with the exception of certain NMR spectra obtained with the sea urchin histone.

Earlier optical rotatory dispersion (ORD) measurements (Bradbury et al., 1965, Jirgensons and Hnilica, 1965) indicated that although H2A was largely in the random coil form in pure water, an increase of ionic strength led to a partial coil → helix transition. We have reinvestigated the formation of secondary structure using CD and Table II

Table II: CD Data for H2A Histone in Aqueous Solution.

	pH	Protein Concn (mg/ml)	$-[\theta]_{222}$ deg cm^2 dmol^{-1}	% Helix	Residues in α Helix
Unbuffered Salt (*M*)					
0.0	3.90	1.0	3,250	8	10
0.0	3.76	5.0	3,940	10	13
0.01 NaCl	3.97	1.0	5,170	14	19
0.025 NaCl	4.00	1.0	5,665	16	21
0.050 NaCl	4.11	1.0	6,160	18	23
0.10 NaCl	4.22	1.0	6,650	19	25
0.25 NaCl	4.40	1.0	7,640	23	30
0.50 NaCl	4.57	1.0	8,375	25	33
1.00 NaCl	5.04	1.0	8,620	26	34
2.00 NaCl	5.69	1.0	9,115	28	36
0.1 NaCl	5.57	0.05	6,850	20	26
0.5 NaCl	6.41	0.05	7,960	24	31
1.0 NaCl	6.71	0.05	8,420	26	33
2.0 NaCl	6.84	0.05	8,430	26	33
Phosphate-buffered salt					
0.1 *M*	2.96	0.05	6,780	20	26
0.1 *M*	4.90	0.05	6,550	19	25
0.1 *M*	6.82	0.05	6,800	20	26
0.1 *M*	8.92	0.05	7,490	22	29
1.0 *M*	2.96	0.05	8,890	27	35
1.0 *M*	6.84	0.05	8,430	26	33
1.0 *M*	8.92	0.05	8,420	26	33
Organic solvent–water mixtures					
80% methanol			16,000	52	67
80% ethanol			17,700	58	74
80% trifluoroethanol			17,700	58	74

lists ellipticities measured at 222 nm under a variety of solution conditions. The very considerable capacity of the molecule for helix formation is illustrated by the results in organic solvents–water mixtures. The general conclusion that follows from these data is that while the helicity is low (though not zero) in water, even small increases in ionic strength lead to a rise in helicity, to a maximum of about 28% or 36 residues. In contrast, changes in pH between 3 and 9 at constant ionic strength have little effect on the helicity.

This helix content is somewhat less than the region predicted by Lewis and Bradbury (1974) (Figure 1) at high salt (47–93, i.e., 47 residues), and that predicted by the two other procedures. It might be that addition of salt induces the formation not of α helix but of β structure, particularly since it is known that this histone aggregates at high ionic strengths. However, the addition of salt induced an increase in negative ellipticity at 222 nm and not at wavelengths in the region of 218 nm. At the highest helicities (0.5–2.0 *M* NaCl) the CD spectrum showed the double negative peaks at 222 and 207 nm characteristic of an α helix–coil mixture. Furthermore, infrared spectra have been obtained in 0.4 *M* phosphate-D_2O buffer (pH 6.9) and compared with that in pure water pH 3. The two spectra appeared identical and showed a broad symmetrical amide 1 band at 1647 cm^{-1}, typical of a random coil–helix mixture in D_2O and no evidence of a band at ~1615 cm^{-1} that would indicate β structures (Miyazawa and Blout 1961, Bradbury and Elliott 1963, Chirgadze et al., 1973). These infrared spectra were obtained using 5% w/v solutions, a concentration much greater than that used for either CD or NMR measurements. It is reasonable to conclude therefore that none of the secondary or aggregative effects observed with the histone at high ionic strength are due to β structure formation.

High resolution NMR spectra have been obtained of H2A using a variety of salts. Figure 2 shows upfield spectral changes occurring on the addition of sodium chloride at a protein concentration of 1 mg/ml, that of the majority of the CD measurements. Certain resonances show clear evidence of intensity reduction on salt addition (assignments from Boublik et al., 1970a): (1) the CH_3 resonance of valine, leucine, and isoleucine at 0.93 ppm; (2) the δ-CH_2 resonance of arginine at 3.2 ppm; (3) the γ-CH_2 resonance of glutamic acid at 2.4 ppm; (4) the δ-CH_2 resonance of proline at 3.7 ppm; (5) the β-CH_2 resonance of aspartic acid and asparagine at 2.9 ppm.

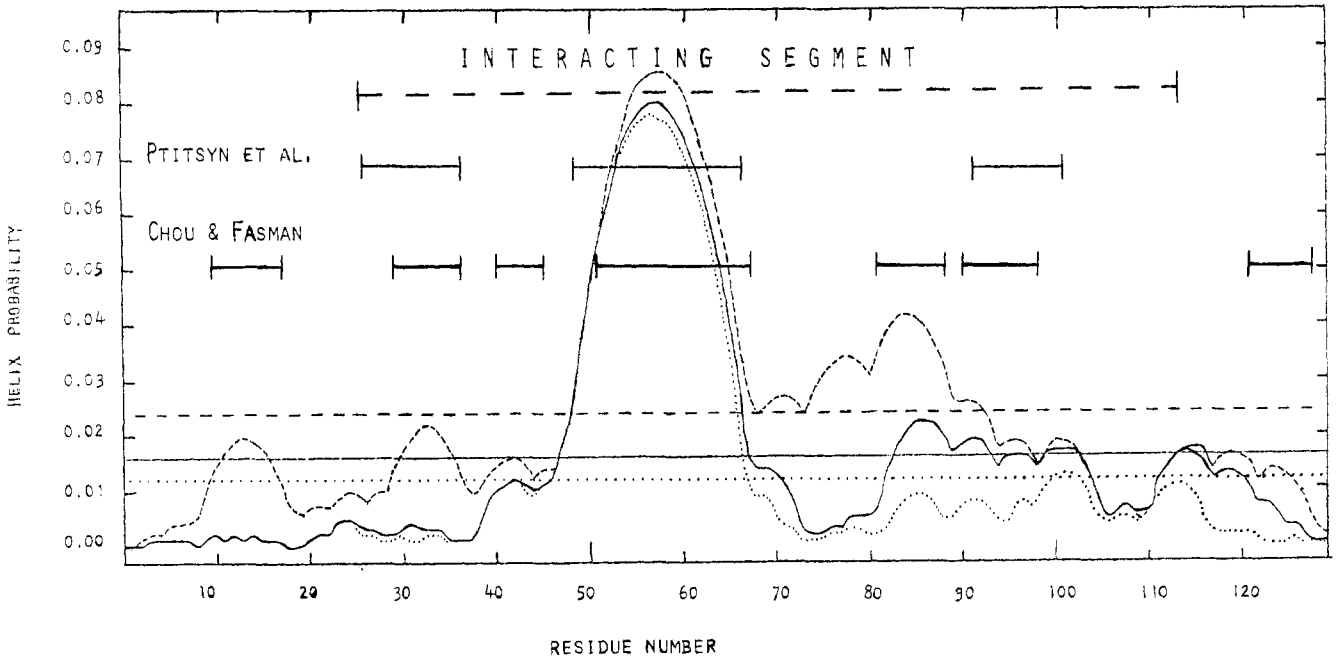

FIGURE 1: Helix probability profile for calf H2A histone: (. . . .) pH 3; (—) pH 7; (- - -) high ionic strength. The horizontal lines represent mean helical probabilities under the same conditions (Lewis and Bradbury, 1974). Also helical segments predicted by two other sets of authors and the region found by the present study to be included in intermolecular aggregates (upper dashed line).

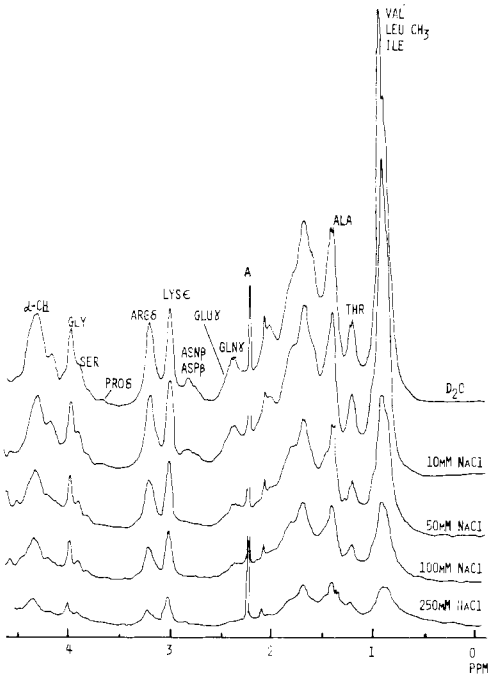

FIGURE 2: Upfield spectrum (270 MHz) of H2A (1 mg/ml, 7×10^{-5} M) in D_2O/NaCl (pH ~4) (FT, 4×10^4 pulses/spectrum; A = acetone).

In contrast, certain other peaks seem less affected: (1) the ϵ-CH_2 resonance of lysine at 3.06 ppm; (2) the CH_3 resonance of threonine at 1.24 ppm; (3) the γ-CH_2 resonance of glutamine at 2.40 ppm; (4) the β-CH_2 resonance of serine at 3.90 ppm.

Two resonances, that of the α-CH_2 of glycine at 3.99 ppm and that of alanine CH_3 at 1.46 ppm (which overlays that of lysine γ-CH_2), are markedly reduced in height although a strong component still remains at 0.25 M NaCl.

The sequence of H2A is presented in Figure 3 on a helical surface. This is firstly a convenient method of sequence presentation and secondly allows an assessment of relative side chain positions but it is *not* implied by this presentation that the whole of the molecule is helical. The sequence of H2A and the data of Table I lead to the conclusion that at high ionic strength it is the N terminal region of the molecule that remains unaffected and possibly also some of the C-terminal portion. This conclusion can be made more precise by a study of the aromatic resonances (Figure 4). It is apparent that even small increases in ionic strength lead to a marked broadening of tyrosine resonance, which also completely disappears at 0.25 M NaCl. All three tyrosine residues are close together (Figure 3) and situated in the second quarter of the molecule, which is the most hydrophobic region of the chain. It is not unexpected that this section of H2A is involved in the interaction since it has a highly hydrophobic nature: between 42 and 73 there is not a single basic residue and the glutamic acid residues will be uncharged at the pH of the experiment (pH ~4). There are four histidine residues in H2A and on salt addition there is some apparent loss in area (Figure 4) of the C_2 proton resonance that appears to correspond to the loss of two histidine resonances. The most reasonable interpretation is that these are histidine-31 and -82 while histidine-123 and -124 remain in an uninteracted and mobile state. H2A contains a single phenylalanine at position 25. At pH ~4 this resonance (7.3 ppm) is overlapped by the C_4 histidine resonance (see Figure 4) but since the histidine C_4 intensity should

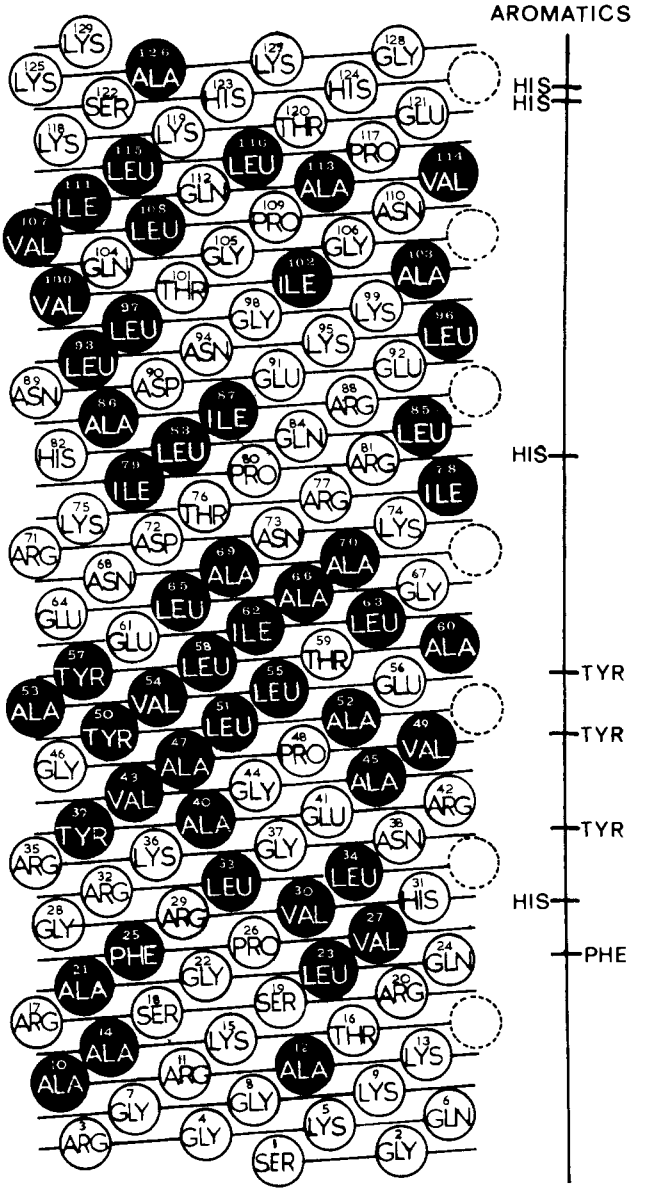

FIGURE 3: Two-dimensional helical surface of calf thymus histone H2A (F2A2).

equal the histidine C_2 intensity one can conclude that at 0.25 M NaCl (pH ~4) the phenylalanine resonance is much broadened. This implies that at the highest ionic strengths the intermolecular interactions extend as far as residue 25.

In order to make a more precise definition of the region of the H2A chain involved in these interactions we have made computer simulations of the spectrum under several conditions using a procedure described previously (Bradbury and Rattle, 1972). Figure 5a and b shows the effects of broadening to 200 Hz resonances from a gradually increasing section of the molecule, commencing at 47–67 (the region predicted to be helical by Lewis and Bradbury, 1974) and continuing to 25–113 (which constitutes ~70% of the whole molecule). Clearly, there is a good match between the predicted changes and the observed spectra (Figures 2 and 4) and it can be concluded with confidence that at high ionic strength the region from about 25 to 113 is involved in intermolecular interactions. This segment of the molecule contains all of the potential for helix formation, see Figure 1 (with the exception of the highly charged sections 9–17

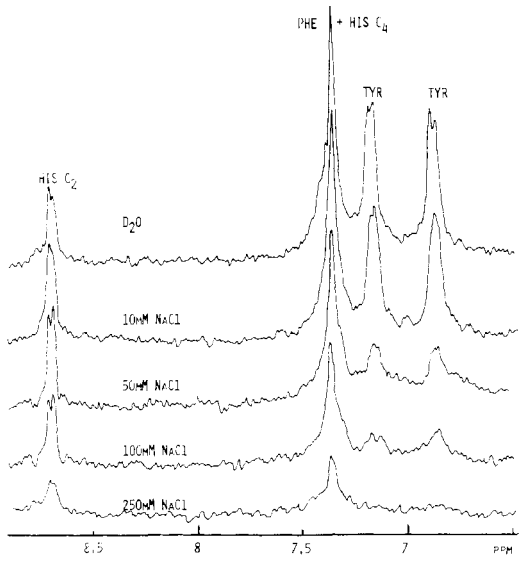

FIGURE 4: Aromatic spectrum (270 MHz) of H2A (1 mg/ml, 7×10^{-5} *M*) in D_2O/NaCl (pH 4) (FT, 4×10^4 pulses/spectrum.).

and 121–127), and it is reasonable to conclude that at high salt all of the helical residues (~36) observed by CD lie within this region. The interacted region is therefore about 40% helical.

The above spectra were obtained at pH ~4 (since this is the pH of the dissolved unbuffered histone) and so we have performed several experiments at neutral pH to confirm that our conclusions remain unaffected by a change to more physiological pH. The first was to titrate a 1 m*M* H2A solution to pH 7: in this unbuffered neutral state no spectral broadening was noted. Results very similar to those at pH ~4 (Figure,2) were obtained. The second experiment was to add 6 *M* urea to an H2A solution in 0.4 *M* phosphate buffer at pH 7.0 to produce an uninteracted state and then reduce the urea concentration in stages to allow the formation of secondary structure and intermolecular interactions since 0.4 *M* phosphate alone is quite sufficient salt to induce this state. The aromatic spectra obtained under these conditions are shown in Figure 6 (lower part) and are very similar to the pH ~4 spectra of Figure 4. It is important to note that in Figure 6 the C_4 resonance of the four histidines lies on top of the lower field component of the tyrosine pair, leaving the single phenylalanine resonance unobscured. It is strikingly clear that not only is phenylalanine-25 reduced in intensity as the urea concentration is lowered and therefore must be involved in the interactions (as previously concluded) but also that two and only two histidines are involved. In order to make a firm assignment of the histidine resonances we have performed two experiments. The first was to cleave the molecule at arginine-88 with trypsin after protecting the lysine residues with maleic anhydride. The peptide 89–129 was then deprotected and the NMR spectrum obtained under identical conditions, viz., 6 *M* urea and 0.4 *M* phosphate. The aromatic spectrum is shown in the upper part of Figure 6 and shows the expected resonance from just two histidine residues (123 and 124) and no phenylalanine or tyrosine. Comparison with the spectrum of the complete molecule demonstrates that the two lower field histidine C_2 resonances can be assigned to 123 and 124. The second experiment was to make use of sea urchin ALG histone which is closely similar to calf thymus H2A (ALK) (Wouters-Tyrou et al., 1974). The major compositional differences are: (1) the sea urchin protein contains more serine and less threonine than the calf protein, (2) in the sea urchin protein there is an additional phenylalanine at position 33 and two of the histidines of calf H2A are missing: those at 123 and 124. Although the full sequence of sea urchin ALG histone

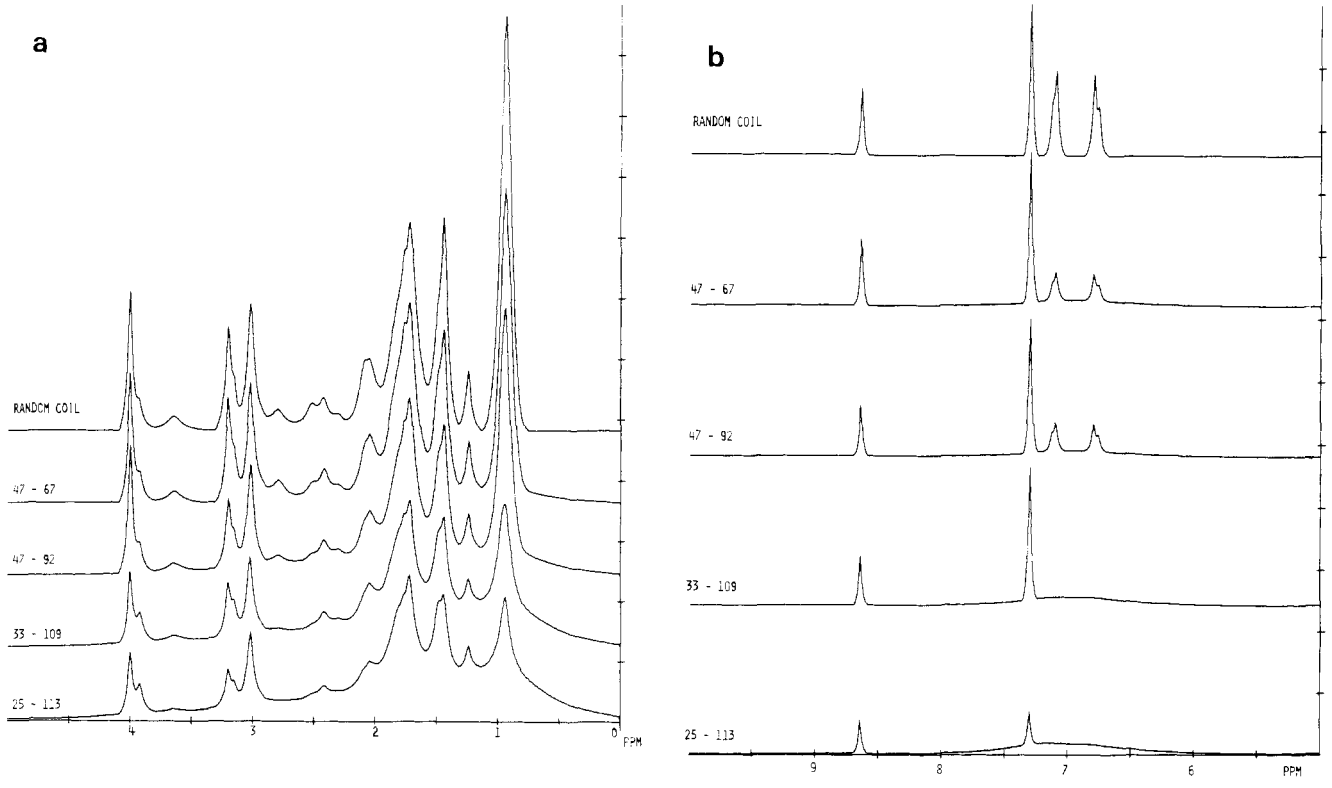

FIGURE 5: (a) Upfield H2A spectra simulated by broadening (to 200 Hz) resonances from a section of chain increasing in stages up to 25–113. (b) Low-field H2A spectra simulated by broadening (to 200 Hz) resonances from a section of the chain increasing in stages up to 25–113.

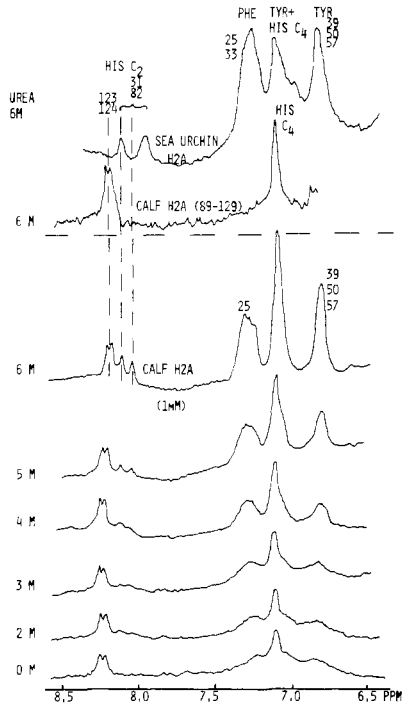

FIGURE 6: Aromatic spectra of H2A (1 mM) in 0.4 M phosphate buffer/D_2O (pH 7.0) with changing urea concentration.

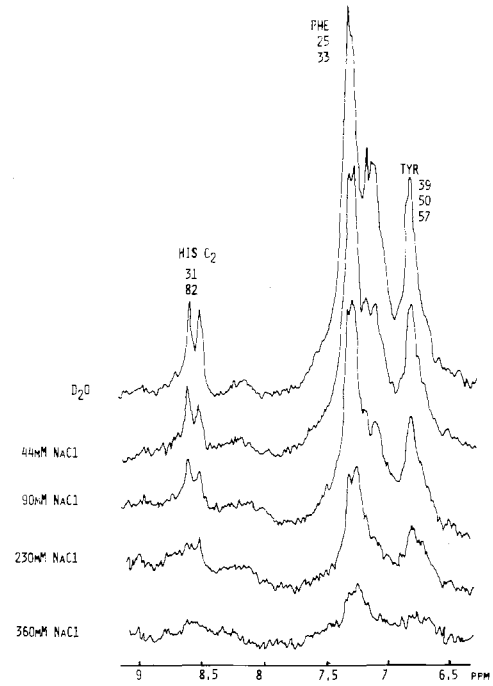

FIGURE 7: Aromatic spectrum of sea urchin H2A (1 mM) pH 3.5 in D_2O/NaCl.

is not yet determined, it is clear that the differences from calf thymus occur largely though not completely in the regions that remain uninteracted on salt addition. The aromatic spectrum of the sea urchin protein in 6 M urea and 0.4 M phosphate is included in Figure 6 and it is apparent that there are two phenylalanines and only two histidines in addition to the three tyrosines. The chemical shift of one of the C_2 histidine protons coincides exactly with that of one of the upfield pair of calf H2A peaks and the other is somewhat upfield of all of the calf peaks. These observations support the assignment of the upfield pair in calf thymus H2A to histidine-31 and -82. We have also checked that the two histidines in the sea urchin protein are both included in the interactions by adding sodium chloride at pH 3.5. Figure 7 shows the resulting spectra and these should be compared with those of calf H2A shown in Figure 4. It is clear that all the aromatic resonance is much broadened on salt addition, in particular both the histidines. These results corroborate the histidine assignments in the calf H2A and also show that the interacted region extends at least from residue 25 to residue 82.

To what precision is it possible to de'ineate the interacted region? Although the spectrum simulation procedure is much more exact than visual inspection of the spectral changes, it is not thought that the interacted region is defined to better than five residues, i.e., 89 ± 5. One limitation of the method is that when deciding which portion of the chain is involved we have restricted ourselves to broadening resonances from a single unbroken sequence of amino acids, largely because it seems unreasonable that two or more interacted, i.e., aggregated regions could be separated by a flexible coil region in so small a protein. In the case of H2A, consideration was given to the possibility that a break between interactions exists in the nonhelix forming and highly charged third quarter of the molecule which includes a concentration of arginine. However, histidine-82, situated in the middle of this region, is observed to lose apparent intensity, and good simulations could not be achieved without the inclusion of the several apolar residues in this region. An unbroken sequence from 25 to 113 was found to give the best fit with the spectra in 0.25 M NaCl.

The model proposed above (and in previous papers from this laboratory, e.g., Bradbury and Rattle, 1972) to explain the structural changes on salt addition involves a gradually increasing portion of the H2A molecule and therefore a series of thermodynamically defined intermediate states. It has been checked that the spectra at different salt molarities shown in Figures 2 and 4 are not a function of the time between salt addition and obtaining the spectrum, i.e., the intermediate stages are not kinetically determined. The characteristic feature of this model is that of the NMR peaks that lose apparent area by broadening, some (such as tyrosine, 2 out of 3 of which are located in the initial 47–67 region) should do so at an ionic strength appreciably lower than that required to broaden, say arginine (δ-CH_2 at 3.2 ppm) which is entirely absent from the 47–67 region. There are, in fact, no basic residues between arginine-42 and arginine-71 and this section is therefore very hydrophobic. Comparison of the aromatic tyrosine and arginine δ-CH_2 peaks (Figures 2 and 4) indicates that they behave very similarly on salt addition, viz., 10 mM NaCl induces only a small loss of apparent area, while 50 mM induces a substantial change. Further salt addition induces a more gradual loss of apparent area in both peaks. Thus both peaks lose apparent intensity together and not at different salt molarities despite the residues being very separated along the polypeptide chain. The spectra at neutral pH (Figure 6) also show simultaneous changes of several residues, viz., phenylalanine-25, histidine-31, tyrosine-39, -50, and -57, and histidine-82; this shows that at least residues 25–82 are simultaneously involved in the intermolecular interactions. The spectra therefore do not indicate that the interacted region gradually spreads along the chain and indeed a scheme of histone folding and aggregation involving numerous intermediate states is not very attractive.

A perhaps more satisfactory model is that the structure

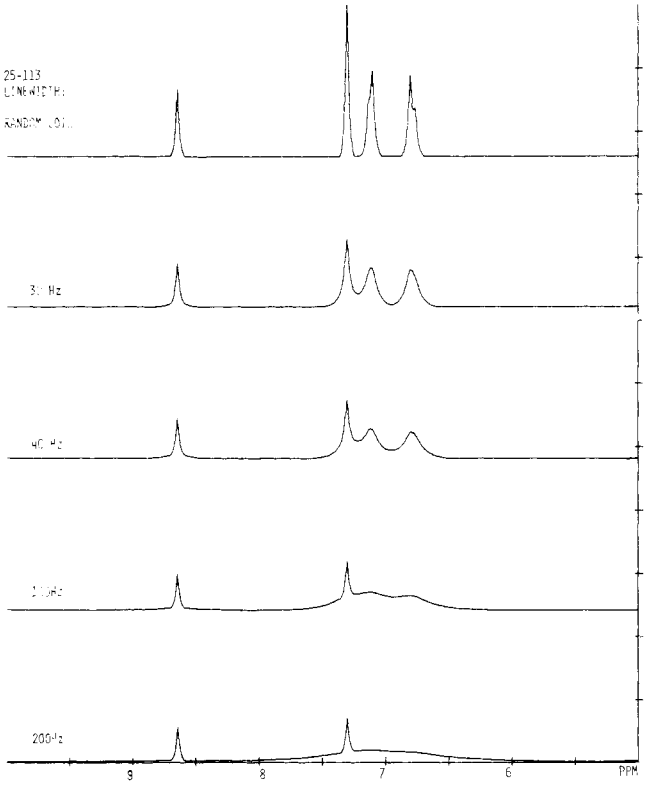

FIGURE 8: Low-field H2A spectra simulated by broadening the section 25–113 in stages from the coil width up to 200 Hz.

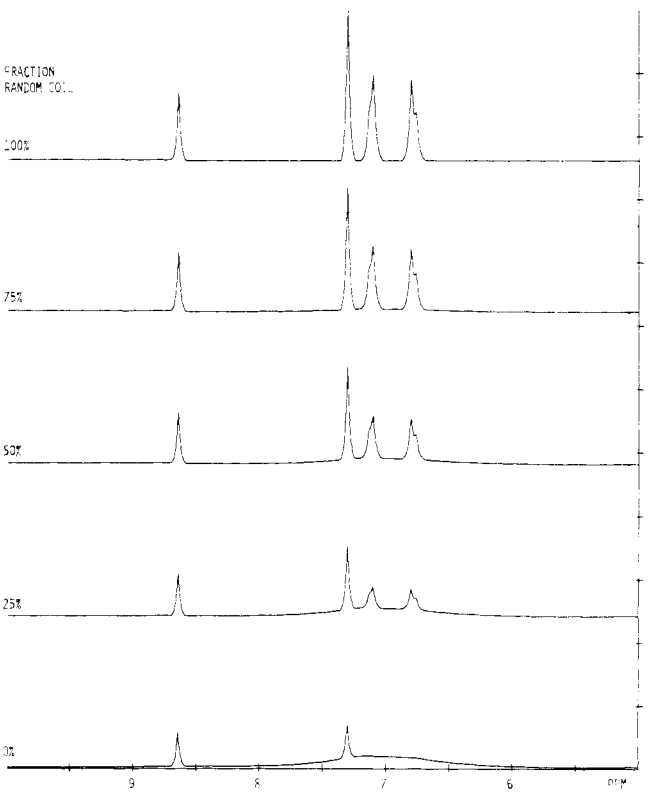

FIGURE 9: Upfield H2A spectra simulated by adding to the coil spectrum an increasing proportion of the spectrum obtained by broadening the section 25–113 to 200 Hz.

always involves the complete region 25–113. Raising the ionic strength might serve to gradually increase the size of the aggregates (as suggested by hydrodynamic data) and so produce a gradually increasing line width. Simulations have therefore been carried out by gradually broadening the region 25–113 to a final width of 200 Hz: the final width being chosen in order to obtain a good fit with the experimental spectrum in 0.25 *M* NaCl. Comparison of the upfield simulations with the observed spectra and with the simulations of the first model leads to no firm preference for either model. This may largely be because all peaks in the upfield spectrum are composite and arise from many residues, only some of which are involved in the structure, and changes in apparent peak intensity therefore lie on a background of unchanged resonance from residues in the unstructured regions. Thus marked differences between the models do not show up. Only when a very small number of residues is involved, e.g., the aromatics, is it possible to establish exactly how the resonances from the interacted region behave. Figure 8 shows the lowfield simulations obtained by this second model and these clearly give a poorer fit to the observed spectra. This conclusion is largely based on the observation that the tyrosine resonance (from three residues closely situated in the molecule) does not gradually broaden on salt addition but appears to lose area such that the width of the remaining line stays approximately constant. It is important to note that a similar spectral effect would be produced if an equilibrium is postulated between structured aggregates of sufficient size to give rise to a line width of at least 200 Hz and random coil molecules—provided that there were rapid exchange on the NMR time scale of molecules between the two states. Such rapid exchange does not, however, seem likely into and out of such an interacted (aggregated) state.

If, however, there were no, or only slow exchange between the interacted state and the coiled state, then the observed spectrum would simply be the sum of a broadened spectrum and the initial sharp spectrum in pure water, with a gradually decreasing contribution from the latter as the ionic strength rose. A set of simulations on this basis has been carried out, with the structured state as before having the resonances of residues 25–113 broadened to 200 Hz. The initial and final simulations are thus the same as in both the previous models (Figures 5 and 8). The upfield simulations are unfortunately not sufficiently different from the previous models to permit a clear preference; however, in the calculated lowfield spectrum (Figure 9) the tyrosine resonance is very well simulated and is clearly an improvement on the second model of a gradually increasing line width. The behavior of the tyrosine resonances is the best test of any model since all three are close together in the molecule and all are included in the structured region. A perfect test can only be provided by observation of single residues and the simultaneous broadening of histidine-31 and histidine-82 (Figure 6) provides the strongest piece of evidence for the rejection of the first model in which the interacted region of the polypeptide gradually increases in size. The final preference is therefore for the last model of an equilibrium between unstructured coil molecules and fully interacted and aggregated molecules.

Influence of Different Salts. It is a common feature of histones that increase in ionic strength promotes the formation of secondary structure and with all except the very lysine-rich histones H1 and H5 aggregation is also induced. The reason for a detailed study of salt induced changes has been the hope of simulating the highly ionic environment of DNA (a macroanion) and of observing biologically important conformations. We have studied the effect of several

salts in order to decide whether the effects are cationic, anionic, or simply the consequence of total ionic strength.

If a plot is made of apparent peak areas against sodium chloride concentration, then one concludes that the major spectral changes have taken place by about 0.2–0.3 *M* NaCl (or $MgCl_2$). Subsequent spectral broadening requires addition of very considerably more NaCl and can be ascribed to very large scale aggregation. At 0.2 *M* NaCl the CD and ORD parameters are not far from their limiting values. For these reasons a comparison was made of the molarities of several salts required to induce changes in the NMR spectrum close to those of 0.2 *M* NaCl. No significant differences were observed between the broadened spectra in different salt solutions (such as might indicate specific effects with certain ions) and the results are shown in Figure 10. It is clear that it is neither the molarity of the added salt nor the overall ionic strength that governs the effects. The quantity that remains very roughly constant is the ionic strength of the anion. In a related way D'Anna and Isenberg (1974) have shown that phosphate is about 20 times more effective than chloride in promoting secondary structure and that magnesium is about equally effective as sodium. It must therefore be an anion effect and comparison between sodium chloride and potassium ferrocyanide (a diamagnetic anion with a charge of −4) is striking: only one-hundredth the quantity of ferrocyanide is required to induce the same effects, an amount that corresponds to only 3 mol of anion/mol of histone. The most reasonable explanation for such an anion effect is that in this very basic protein the strong chaotropic effects of the many lysine and arginine residues are markedly reduced by effective counterion screening, leading to secondary conformations, folding, and aggregation.

If such counterion screening is all important then it might be that there is a critical region of the H2A molecule at which strong anion binding immediately leads to structure formation over a considerable length of the chain. We have therefore investigated the effects of two paramagnetic anions to look for any evidence of specific anion binding. The chromicyanide ion $Cr(CN)_6^{3-}$, having a relatively slow electron relaxation time, gives rise to strong broadening effects. At 1 m*M* protein concentration, 0.1 m*M* chromicyanide gave rise to a perceptible broadening. At 1 m*M* chromicyanide, probably not sufficient to induce much interaction, considerable broadening of the protein spectrum was produced, but there was no evidence that the arginine and lysine resonances were any more affected than say the glycine, glutamic acid, or the apolar resonances, i.e., the broadening effects of the anion were spread over a considerable region of the molecule. It was, however, clear that the anion does bind to the protein and the broadening is not simply due to free chromicyanide in solution, from the fact that no broadening was observed in the peaks of a very small amount of added ethanol.

As a further check on the possibility of specific anion binding, the ferricyanide ion $Fe(CN)_6^{3-}$ was used. This has a short electron relaxation time and is primarily a shift inducer. At 2 m*M* and greater concentrations of ferricyanide the spectrum showed some broadening and was very similar to that observed at a similar concentration of the diamagnetic ferrocyanide: this must be a consequence of the formation of the interacted state. However, there was no sign of any shifted peaks, e.g., of lysine or arginine, as would indicate strong and specific binding of ferricyanide. The general conclusion is therefore that anion shielding of basic

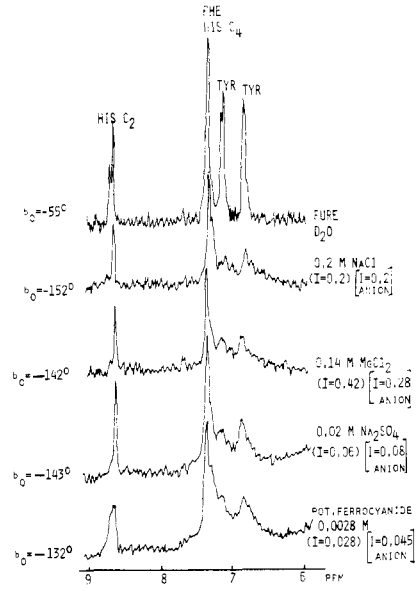

FIGURE 10: Aromatic spectrum (270 MHz, FT) of histone H2A (1 m*M*) at pH 3, in D_2O with different salts at concentrations giving rise to a similar spectral broadening.

residues without high specificity is responsible for the interactions. It would also be reasonable to conclude that it is shielding of basic residues in the 25–113 section of the molecule that is the primary effect, rather than shielding in the more basic N and C terminal regions of the molecule. There is, however, no direct evidence for preferential interaction of anions with the central region of the molecule.

Interaction with DNA. If the section 25–113 takes part in interhistone interactions, then the remainder of the molecule, which is strongly basic, is probably the site of interaction with DNA. It is striking that from arginine-3 to arginine-17 every alternate residue is basic, with the single exception of glycine-7. In an extended conformation all these basic residues would be on the same side of the protein molecule as shown in Figure 11 and very appropriately situated for regular interaction with the negative phosphate groups of the DNA. It may also be significant that the residues which alternate with the basic residues are either helix destabilizing, e.g., glycine or serine, or contain short side chains, e.g., alanine. These residues are found widely in the extended chains of silks. A similar situation obtains in the basic carboxyl end of the molecule and thus the amino acid arrangement in both terminal regions is in marked contrast to that of the central region which is observed to take part in intermolecular interactions.

We have investigated the H2A/DNA interaction by adding a solution of H2A at 5 mg/ml in 5 *M* urea and 2 *M* salt to a solution of calf thymus DNA at 15 mg/ml under the same conditions. By stepwise dialysis the salt concentration was first reduced to zero and the urea concentration was subsequently reduced to zero by the same procedure. At this stage no NMR spectrum could be seen and the histone was judged to be tightly bound to the DNA and completely immobilized. The salt molarity was then increased to 0.8 *M*, a concentration at which H2A starts to be released from chromatin and from the reconstituted complex. At this point of the dissociation of H2A from DNA, the released portion of the histone chain may take part in interhistone interactions which broaden resonances from the amino acids located there: the protein spectrum is thus broadened

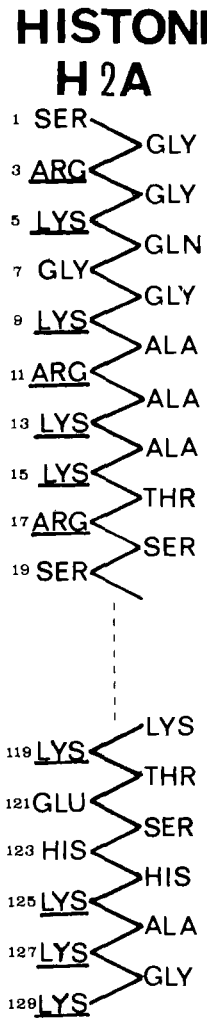

FIGURE 11: The N-terminal and C-terminal regions in an extended structure showing the regular arrangement of basic residues.

throughout. If the protein/DNA ratio is kept low, however, then this situation can be largely avoided. Reconstitution procedures were thus carried out at low protein/DNA ratios. Figure 12 shows a comparison of the spectrum of H2A alone in 0.6 *M* NaCl and in the presence of DNA at 0.8 *M* NaCl. The upper spectrum is very similar to that of H2A in 0.25 *M* NaCl in Figure 2 and in fact there is little change in the H2A spectrum between 0.25 and 0.8 *M* NaCl. In the presence of DNA a completely different spectrum results in which certain resonances that are markedly broadened by histone–histone interactions in the upper spectrum have become sharper and more prominent: the valine, leucine, and isoleucine CH_3 peak at 0.92 ppm, the glutamic acid and glutamine γ-CH_2's at 2.4–2.5 ppm, and the tyrosine resonances at 6.8 and 7.1 ppm. It follows that the central portion of the molecule has become free under these conditions. Conversely, the resonances from the basic residues, for example, arginine δ-CH_2 and lysine ϵ-CH_2 at 3.2 and 3.0 ppm, respectively, are much reduced in apparent intensity: the same is true of the histidine resonances at 7.2 and 8.6 ppm. In other words, the basic portions of the molecule that remain are free when histone–histone interactions induced by salt have become preferentially bound to DNA and therefore broaden, while the central apolar regions of the histones do not aggregate under these conditions but remain free and give rise to a sharp spectrum.

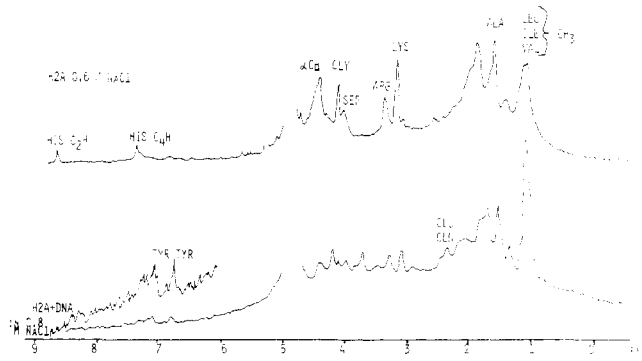

FIGURE 12: Comparison of spectra of H2A in 0.6 *M* NaCl (pH 6.5) and H2A + DNA (weight ratio, 1:3) in 0.8 *M* NaCl (pH 6.5). H2A concentration 3 mg/ml.

Discussion

The addition of salt to H2A solutions results in instantaneous changes in the secondary structure that can be assigned to helix formation on the basis of negative maxima at 204 and 222 nm. The ellipticities observed in this work are in good agreement over the full wavelength range of 190–260 nm with those reported in a very recent study of D'Anna and Isenberg (1974). Those authors have taken the ellipticity of H2A in water at pH 4 as the coil reference ($[\theta]_{222} \approx -2800°$) although there is a discernible negative peak at 222 nm in this spectrum. However, on the addition of 8 *M* urea to a solution in water there is a sharpening of the NMR spectrum and a change in the optical rotation $[R']_{233}$ from −3300 to −2200° (Bradbury et al., 1968; Hnilica, 1972, p 53), corresponding to a reduction in helicity of ~9% on an $[R]_{233}$ scale of: coil = −1740°, helix = −13,800° (Chen et al., 1974). We have therefore taken the view that H2A retains some helicity in water. This is supported by the observation that when H2A is dissolved in D_2O at 5 mg/ml ($[\theta]_{222} = -3940°$) a proportion of peptide NH hydrogens exchanges more slowly than the majority. Hvidt and Nielson (1966) indicate a half-life of about 7 min for a random coil peptide hydrogen in D_2O at pH ~3.5. For H2A, however, after 45 min in D_2O, 12 ± 3 protons remain unexchanged ($\tau_{1/2}$ = 7 min implies 0.2 proton remaining after 45 min). If some helix does indeed remain in water, what then is the ellipticity of fully coiled H2A? Chen et al. (1974) suggest a value of +1580° at 222 nm while a survey of globular proteins in 6 *M* guanidine hydrochloride (Cortijo et al., 1973) suggests a negative value in the region of −1000°. Faced with the uncertainly we have attempted to use histone molecules and their cleaved fragments as random coil models. Comparison of the CD of several such molecules in water shows that whereas all the calf thymus histones (including H1) show a significant though small negative inflexion at 222 nm, a C-terminal peptide of H1 (107–217) does not (this peptide is very basic and contains 40% lysine, 30% alanine, and 14% proline). Two peptides from calf thymus H4 behave likewise: H4 (1–23) is also very basic and contains 35% glycine whereas H4 (69–102) is much more hydrophobic in character (Lewis et al., 1974). All three molecules exhibited an ellipticity at 222 nm between −400 and −1500°. On the assumption that these three molecules of very differing composition are all completely random coil or very nearly so, an average coil ellipticity at 222 nm of −1000° was used to compute H2A helicities. This value implies of course a residual helicity in pure water. The pure helix ellipticity at 222 nm was taken as

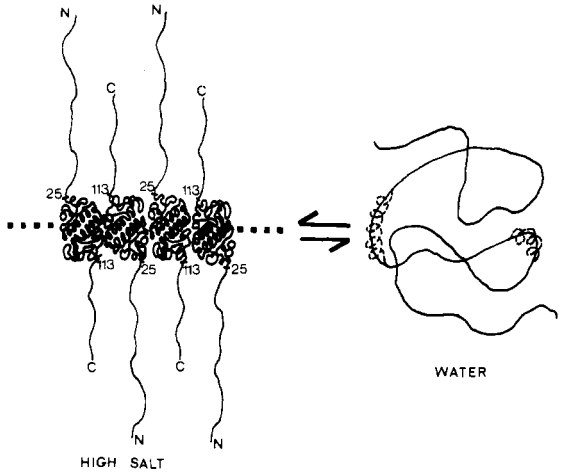

FIGURE 13: Schematic representation of the folding of histone H2A. The residual helix in water is represented by a dotted line.

$-30{,}000°$, a figure derived by Chen et al. (1974) from an analysis of five globular proteins and shown by them to be appropriate to helices of average length about 12 residues. This value seems more reasonable for a small protein molecule than $[\theta]_{222} = -35{,}500°$ (Greenfield and Fasman, 969) which Chen et al. (1974) show to be appropriate to helices of average length about 20 residues. Our choice of reference ellipticities leads to the present estimates of helicity being about 15% greater than those of D'Anna and Isenberg for the same measured ellipticity of about $-8500°$ in high salt. An important question is the location of any helix and whether it is present as a single length of about 35 residues or is interspersed with coil regions. The helical predictions in Figure 1 do not suggest a single continuous stretch of helix, although D'Anna and Isenberg (1974) using the predictive statistics of Kabat and Wu (1973) propose 85–105 as the helical region. Unfortunately, on the present data it is not possible to define the position of any helix, since helix formation (monitored by CD) appears always to be immediately accompanied by intermolecular interactions (monitored by NMR) and the NMR spectrum is not capable of indicating which of the broadened resonances is actually located in a helix. Only the study of cleaved peptides from H2A can directly answer the question as to the location of any helical segments.

A generalized scheme for the salt induced conformational changes and interactions in histone H2A is given in Figure 13. Residues 47–66 and 78–88 are taken to be in the α-helical conformation; this is in rough accord both with the number of α_R residues observed by CD and with the predictions of Lewis and Bradbury (1974) that show two peaks of high helix probability (Figure 1). The present measurements show that on salt addition the formation of secondary structure (CD) and intermolecular interactions (NMR) take place simultaneously. Essentially the same observation has been made by D'Anna and Isenberg (1974) who monitored the intermolecular effects from the anisotropy of tyrosine fluoresence (although the use of this technique restricts any conclusions to the region 39–57 where the three tyrosines lie). Figure 13 therefore incorporates the concept that molecules containing considerable secondary structure do not exist unassociated. Also included is the finding that the whole of the region 25–113 is simultaneously incorporated into the intermolecular associates.

In the interaction of histones H2A with DNA the associated state of the histone is disrupted by the stronger binding of the basic regions to DNA. This presumably partially destabilizes the structured region of H2A, allowing it to have sufficient mobility to give a well-developed NMR spectrum at intermediate salt molarities. At lower salt molarities the whole of the H2A molecule becomes tightly bound, while at high salt it is fully dissociated and self-associates.

References

Boublik, M., Bradbury, E. M., and Crane-Robinson, C. (1970a), *Eur. J. Biochem. 14,* 486.

Boublik, M., Bradbury, E. M., Crane-Robinson, C., and Johns, E. W. (1970b), *Eur. J. Biochem. 17,* 151.

Bradbury, E. M., Crane-Robinson, C., Goldman, H., Rattle, H. W. E., and Stephens, R. M. (1968), in Solution Properties of Natural Polymers, London, The Chemical Society.

Bradbury, E. M., Crane-Robinson, C., Phillips, D. M. P., Johns, E. W., and Murray, K. (1965), *Nature (London) 205,* 1315.

Bradbury, E. M., and Elliott, A. (1963), *Polymer 4,* 47.

Bradbury, E. M., and Rattle, H. W. E. (1972), *Eur. J. Biochem. 27,* 270.

Chen, Y.-H., Yang, J. T., and Chau, K. H. (1974), *Biochemistry 13,* 3350.

Chirgadze Yu. N., Shestopalov, B. V., and Venyaminov S. Yu. (1973), *Biopolymers 12,* 1337.

Chou, P. Y., and Fasman, G. D. (1974), *Biochemistry 13,* 222.

Cortijo M., Panijpan B., and Gratzer, W. B. (1973), *Int. J. Peptide Protein Res. 5,* 179.

Croft, L. A. (1973), in Handbook of Protein Sequences, Oxford, Joynson-Bruvvers.

D'Anna, J. A., and Isenberg, I. (1974), *Biochemistry 13,* 2093.

Greenfield, N., and Fasman, G. D. (1969), *Biochemistry 8,* 4108.

Hnilica, L. S. (1972), The Structure and Biological Function of Histones, Cleveland, Ohio, Chemical Rubber Publishing Co.

Hvidt, H., and Nielsen, S. (1966), *Adv. Protein Chem. 21,* 287.

Jirgensons, B., and Hnilica L. S. (1965), *Biochim. Biophys. Acta 109,* 241.

Johns, E. W. (1964), *Biochem. J. 92,* 55.

Johns, E. W. (1967), *Biochem. J. 105,* 611.

Kabat, E. A., and Wu, T. (1973), *Biopolymers 12,* 751.

Lewis, P. N., and Bradbury, E. M. (1974), *Biochim. Biophys. Acta 336,* 153.

Lewis, P. N., Bradbury, E. M., and Crane-Robinson C. (1975), *Biochemistry,* submitted.

Lewis, P. N., Scheraga, H. A. (1971), *Arch. Biochem. Biophys. 144,* 576.

Miyazawa, . T., and Blout, E. R. (1961), *J. Am. Chem. Soc. 83,* 712.

Ptitsyn, O. B., Lim, V. I., and Finkelstein, A. V. (1973), *Anal. Simul. Biochem. Syst., Fed. Eur. Biochem. Soc. Meet., 8th,* 421.

Sautière, P., Tyrou, D., Laine, B., Mizon, J., Ruffin, P., and Biserte, G. (1974), *Eur. J. Biochem. 41,* 563.

Wouters-Tyrou, D., Sautière, P., and Biserte, G. (1974), *Biochim. Biophys. Acta 342,* 360.

Yeoman, L. C., Olson, M. O. J., Sugano, N., Jordan, J. J., Taylor, C. W., Starbuck, W. C., and Busch, H. (1972), *J. Biol. Chem. 247,* 6018.